

A SULPHIDE-CAPACITY PREDICTION MODEL OF BLAST-FURNACE SLAG

MODEL ZA NAPOVEDOVANJE SULFIDNE KAPACITETE PLAVŽNE ŽLINDRE

Yongchun Guo, Fengman Shen*, Haiyan Zheng, Shuo Wang, Xin Jiang,
Qiangjian Gao

School of Metallurgy, Northeastern University, Shenyang 110819, China

Prejem rokopisa – received: 2021-05-11; sprejem za objavo – accepted for publication: 2021-08-02

doi:10.17222/mit.2021.157

A sulphide-capacity prediction model of CaO-SiO₂-MgO-Al₂O₃ slags was developed based on the ion and molecule coexistence theory (IMCT). The biggest advantage of the theoretical model of ion and molecule coexistence was the fact that it is easily popularized and applied within a multicomponent slag system. The sulphide capacity (*C_s*) of the slag for a blast furnace (BF) with high Al₂O₃ in the CaO-SiO₂-MgO-Al₂O₃ system at 1773 K was measured by applying the slag-metal equilibrium method. The feasibility of the developed IMCT model was verified with the sulphide capacity measured during the experiment. The effects of *R* (w/% (CaO)/w/% (SiO₂)), w/% (MgO)/w/% (Al₂O₃) and w/% (Al₂O₃) on the sulphide capacity were discussed. There is a good linear relationship between the experimental values and predicted values. Therefore, the theoretical model of ion and molecule coexistence can be used to calculate the sulphide capacity of a CaO-SiO₂-MgO-Al₂O₃ quaternary slag system. When the amount of Al₂O₃ is 20 w/% and w/% MgO/w/% Al₂O₃ is 0.5, the sulphide capacity of the slag increases with an increase in *R*. When the amount of Al₂O₃ is 20 w/% and *R* = 1.30, the sulphide capacity of the slag increases with an increase in w/% MgO/w/% Al₂O₃. When *R* = 1.30 and w/% MgO/w/% Al₂O₃ = 0.4, the sulphide capacity of the slag decreases with an increase in w/% Al₂O₃.

Keywords: blast furnace (BF), sulphide capacity (*C_s*), mass action concentrations, the ion and molecule coexistence theory (IMCT)

V članku je opisan razvoj modela za napoved sulfidne kapacitete (zmožljivosti) žlindre na osnovi CaO-SiO₂-MgO-Al₂O₃, ki temelji na teoriji koeksistence (sobivanja) ionov in molekul (IMCT; angl.: ion and molecule coexistence theory). Največja prednost tega teoretičnega modela je, da predpostavlja sobivanje ionov in molekul v raztaljeni žlindri, kar se lahko učinkovito uporablja za simulacijo dogajanj v večkomponentnih sistemih žlinder. Merjena je bila sulfidna kapaciteta plavžne žlindre (*C_s*) z visoko vsebnostjo Al₂O₃ v sistemu CaO-SiO₂-MgO-Al₂O₃ pri 1773 K, z uporabo metode ravnotežja med kovino in žlindro. Avtorji so izdelali IMCT model z eksperimentalnim merjenjem sulfidne kapacitete tudi ovrednotili in verificirali. Razpravljali so tudi o posameznih vplivih masnih razmerij *R* (w/% (CaO)/w/% (SiO₂)) in w/% (MgO)/w/% (Al₂O₃) ter masne vsebnosti w/% (Al₂O₃) na sulfidno kapaciteto žlindre. Dobili so dobro linearno povezavo med eksperimentalnimi vrednostmi in vrednostmi, ki jih napoveduje model. Zato se sklepa, da je razviti teoretični model ionske in molekularne koeksistence možno uspešno uporabiti za izračune sulfidne kapacitete kvaternarnih plavžnih žlindernih sistemov tipa CaO-SiO₂-MgO-Al₂O₃. Pri vrednostih 20 w/% (Al₂O₃) in w/% (MgO)/w/% (Al₂O₃) = 0,5 je sulfidna kapaciteta žlindre naraščala z naraščajočim *R*. Ko je bil w/% (Al₂O₃) enak 20 in *R* = 1,30 je sulfidna kapaciteta naraščala z naraščajočim w/% (MgO)/w/% (Al₂O₃). Ko sta bila *R* = 1,30 in w/% (MgO)/w/% (Al₂O₃) = 0,4 pa se je sulfidna kapaciteta zmanjševala z naraščajočo vsebnostjo w/% (Al₂O₃).

Ključne besede: plav (BF), sulfidna kapaciteta (*C_s*), koncentracije masne aktivnosti, teorija koeksistence ionov in molekul (IMCT)

1 INTRODUCTION

Sulphur can harm steel products.¹⁻⁴ Therefore, it is necessary to remove it from molten steel in order to improve its mechanical properties. The sulphide distribution between slags and hot metal is a common parameter for describing the desulphurization during a blast-furnace ironmaking process.^{2,5,6}

Many researchers tried to measure the sulphide capacity of slags for a blast furnace in the CaO-SiO₂-MgO-Al₂O₃ system. X. D. Ma et al. measured the sulphide capacity of the CaO-SiO₂-MgO-Al₂O₃ quaternary system at temperatures from 1773–1823 K with a gas-slag equilibration method, focusing on a low MgO

concentration of BF slags.^{7,8} Seo et al. also measured the sulphide capacity of the CaO-SiO₂-MgO-Al₂O₃ slags at 1773 K using the gas-slag equilibrium technique.⁹ Even though many researchers investigated the sulphide capacity of blast-furnace slag, there is little experimental data regarding high Al₂O₃ in the CaO-SiO₂-MgO-Al₂O₃ system. Beside the experimental data reported on the sulphide capacity, there are also some empirical models such as Young's model,¹⁰ Sommerville's model,¹¹ the KTH model,^{12,13} Reddy's model¹⁴ and IMCT model.^{15,16} However, the developed sulphide-capacity prediction models can only be successfully applied to some slags, without being widely accepted from the viewpoint of metallurgical physico-chemistry.

Based on the theory of ion and molecule coexistence, a thermodynamic sulphide-capacity prediction model for

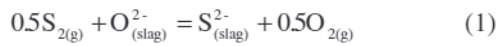
*Corresponding author's e-mail:
shenfm@mail.neu.edu.cn (Fengman Shen)

the CaO-SiO₂-MgO-Al₂O₃ blast-furnace slag and molten iron was established by calculating the mass concentration of a structure unit or ion pair. The model was also validated using experimentally determined sulphur capacities of CaO-SiO₂-MgO-Al₂O₃ slags, with a view to establish a thermodynamic sulphur-capacity prediction model relating to slags and iron. In addition, effects of *R* (w/% (CaO)/w/% (SiO₂)), w/% (MgO)/w/% (Al₂O₃) and w/% (Al₂O₃) on the sulphur capacity were discussed to provide theoretical guidance for a blast-furnace operation.

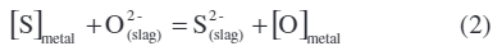
2 EXPERIMENTAL PART

2.1 Experimental principle

The equilibrium reaction of sulphur between the gas and slag phases can be represented with Equation (1):



The equilibrium reaction of sulphur between the metal and slag phases can be represented with Equation (2):



Sulphur distribution between slag and metal can be correlated with the sulphide capacity by combining Equations (1) and (2) as Equation (3):



$$\log K_s = -935/T + 1.375^{17} \quad (4)$$

The sulphide capacity is defined as follows:

$$C_s = (\%S) \cdot \left(\frac{p_{O_2}}{p_{S_2}} \right)^{1/2} \quad (5)$$

The sulphur distribution ratio *L_s* is defined as follows:

$$L_s = \frac{(\%S)}{[S]} \quad (6)$$

The equilibrium constant *K_s* can also be expressed as follows:

$$K_s = \left(\frac{a_o}{a_s} \right) \cdot \left(\frac{p_{O_2}}{p_{S_2}} \right)^{1/2} = \left(\frac{(\%S)}{[S]} \right) \cdot \left(\frac{a_o}{f_s \cdot C_s} \right) = L_s \left(\frac{a_o}{f_s \cdot C_s} \right) \quad (7)$$

where *a_o* and *a_s* are the activities of oxygen and sulphur in the slag, respectively. *p_{O₂}* and *p_{S₂}* are the partial pressures of oxygen and sulphur, respectively (atm). (%S) is the concentration of sulphur in the slag, [S] is the concentration of sulphur in the molten iron and *f_s* is the Henrian activity coefficient of sulphur dissolved in the hot metal. The oxygen activity in the hot metal can be calculated by choosing the equilibrium of the CO/C pairs.¹⁵

According to Equation (7), the expression for the sulphide capacity can be obtained as Equation (8):

$$C_s = L_s \cdot \left(\frac{a_o}{K_s \cdot f_s} \right) \quad (8)$$

The sulphide capacity can also be written as Equation (9):

$$\lg C_s = \lg L_s + \lg a_o - \lg K_s - \lg f_s \quad (9)$$

The activity coefficient of sulphur in the metal can be calculated as follows:

$$\lg f_s = \sum e_s^j [\%j] \quad (10)$$

Where *e_s^j* is the interaction parameter of species *j* on *S* in the molten iron, [%*i*] is the element concentration in the hot metal. The interaction parameters are shown in **Table 1**. **Figure 1** shows a schematic diagram of a desulfurization reaction.

Table 1: Values of interaction parameters^{15,17}

<i>e_c^c</i>	<i>e_c^o</i>	<i>e_c^s</i>	<i>e_s^s</i>	<i>e_s^c</i>	<i>e_s^o</i>	<i>e_o^s</i>	<i>e_o^c</i>	<i>e_o^o</i>
0.049	0.00	0.034	-0.028	0.083	0.0	-0.133	0.00	-0.140

2.2 Experimental procedure

A schematic diagram of the experimental set-up is shown in **Figure 2**. A vertical resistance furnace was used for the equilibration between the CaO-SiO₂-MgO-Al₂O₃ slag and the hot metal at 1773 K. The temperature fluctuation of the furnace was controlled within ± 2 K using an installed B-type thermocouple and a proportional integral differential controller. In the experiment, the iron in a graphite crucible came from a steel plant. The chemical composition of the iron used in this study is shown in **Table 2**. The raw materials, Al₂O₃, CaO, MgO, and SiO₂ powders, were dried at 1273 K for 6 h to remove the moisture. The slags were prepared from a mixture of reagent-grade CaO, SiO₂, Al₂O₃ and MgO. Slag compositions were designed to include *R* from 1.05 to 1.35, w/% (MgO)/w/% (Al₂O₃) from 0.25 to 0.55 and w/% (Al₂O₃) from 12 % to 20 %, respec-

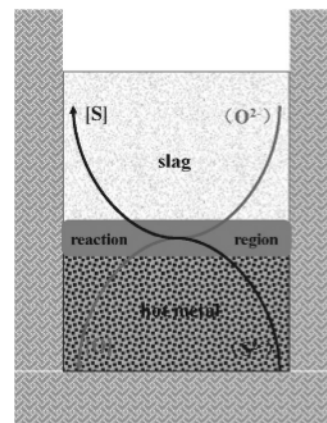


Figure 1: Schematic diagram of a desulfurization reaction

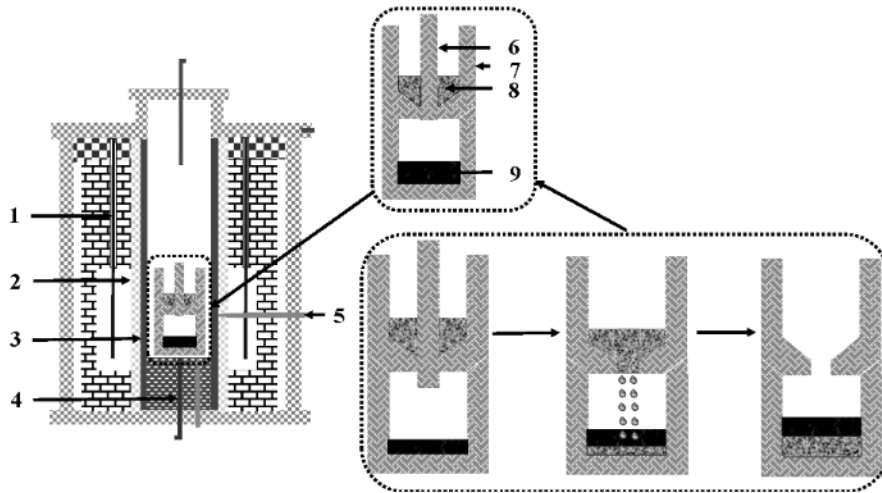


Figure 2: Experimental apparatus: 1 – heating unit of MoSi₂, 2 – Al₂O₃ tube, 3 – graphite tube, 4 – Ar gas, 5 – 30%Rh/Pt-60%Rh, 6 – graphite screw rod, 7 – graphite crucible, 8 – pig iron, 9 – slag

tively. The experimental slag compositions with sulphide capacities are presented in Table 3. The equilibrium times were (30; 60; 90; 120) min. The relationship between the sulphur content in the molten iron and desulfurization time is shown in Figure 3. It is clear from this figure that when the experimental time was more than 80 min, the slag could reach equilibrium with the gas atmosphere. The equilibrium time was determined to be 90 min. The iron and slag were weighed in a ratio of 3:1. When the temperature rose to 1773 K, the iron samples were put in the lower crucible and kept there for 90 min. The samples were directly quenched in oil after the equilibration. All the samples were subjected to a chemical analysis with the PE Avio 500 inductively coupled plasma-atomic emission spectrometry (ICP-AES).

Table 2: Chemical composition of iron/w/%

C	Si	P	S	Mn	Fe
4.63	0.260	0.104	0.105	0.229	94.672

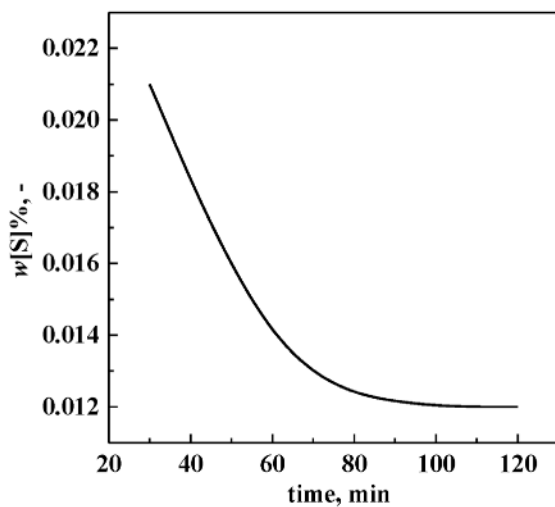


Figure 3: Relationship between the sulphur content in molten iron and desulfurization time

Table 3: Chemical composition of slag/w/%

No.	Slag compositions				R /-	w(MgO)/w(Al ₂ O ₃) /-
	CaO	SiO ₂	MgO	Al ₂ O ₃		
1#	47.02	36.17	4.8	12	1.30	0.40
2#	44.65	34.34	6.0	15	1.30	0.40
3#	42.27	32.52	7.2	18	1.30	0.40
4#	40.69	31.30	8.0	20	1.30	0.40
5#	35.85	34.14	10.0	20	1.05	0.50
6#	37.51	32.49	10.0	20	1.15	0.50
7#	38.89	31.11	10.0	20	1.25	0.50
8#	40.21	29.78	10.0	20	1.35	0.50
9#	42.39	32.60	5.0	20	1.30	0.25
10#	41.26	31.73	7.0	20	1.30	0.35
11#	40.13	30.86	9.0	20	1.30	0.45
12#	39.00	30.00	11.0	20	1.30	0.55

3 SULPHIDE-CAPACITY MODELS

The ion and molecule coexistence theory (IMCT) was applied to predict the sulphide capacity for the CaO-SiO₂-MgO-Al₂O₃ blast furnace slags and hot metal.

3.1 Assumptions based on the coexistence theory regarding the slag structure

Based on the ion and molecule coexistence theory, the following assumptions were made:¹⁸

(1) Molten slag is composed of simple ions such as Ca²⁺, Mg²⁺, O²⁻, etc., simple molecules such as Al₂O₃, SiO₂ and complicated molecules such as silicates, aluminates, etc.

(2) Dynamic equilibrium occurs when ion couples are generated from simple ions and simple molecules form complicated molecules.

(3) Structural units in the selected slags equilibrated with molten iron bear continuity in the investigated concentration range.

(4) Chemical reactions of the formed complex molecules obey the mass action law.

The coexistence theory regarding the slag structure provides a method for calculating the activities of multi-component slag systems.

3.2 Model for calculating the mass action concentrations of the structural units from CaO-SiO₂-MgO-Al₂O₃ slag melts

According to the ion and molecule coexistence theory, there are three simple ions, Ca²⁺, Mg²⁺ and O²⁻, and two simple molecules, SiO₂ and Al₂O₃, in CaO-SiO₂-MgO-Al₂O₃ slags. In accordance with the reported phase diagrams¹⁹ of MgO-SiO₂, CaO-SiO₂, CaO-Al₂O₃, MgO-Al₂O₃, CaO-MgO-SiO₂ and CaO-Al₂O₃-SiO₂ slags at the metallurgical temperature, 18 kinds of complex molecules are listed in **Table 4**.

The mole numbers of the above-mentioned four components, CaO, SiO₂, MgO, Al₂O₃ of CaO-SiO₂-MgO-Al₂O₃ slags, are determined as $n_1 = \sum n_{CaO}$, $n_2 = \sum n_{SiO_2}$, $n_3 = \sum n_{MgO}$ and $n_4 = \sum n_{Al_2O_3}$ for the present chemical compositions of the slags.

$$n_1 = x_1 + x_7 + 2x_8 + 3x_9 + x_{12} + 12x_{13} + 3x_{14} + x_{15} + x_{16} + 2x_{17} + x_{18} + x_{20} + 3x_{21} + x_{22} + 2x_{23} = \sum X(0.5N_1 + N_7 + 2N_8 + 3N_9 + N_{12} + 12N_{13} + 3N_{14} + N_{15} + N_{16} + 2N_{17} + N_{18} + N_{20} + 3N_{21} + N_{22} + 2N_{23}) \tag{11}$$

$$n_2 = x_2 + x_7 + x_8 + x_9 + x_{10} + x_{11} + x_{17} + 2x_{18} + 2x_{19} + x_{20} + 2x_{21} + 2x_{22} + 2x_{23} = \sum X(N_2 + N_7 + N_8 + N_9 + N_{10} + N_{11} + N_{17} + 2N_{18} + 2N_{19} + N_{20} + 2N_{21} + 2N_{22} + 2N_{23}) \tag{12}$$

$$n_3 = x_3 + x_{10} + 2x_{11} + x_{20} + x_{21} + x_{22} + x_{23} + x_{24} = \sum X(0.5N_3 + N_{10} + 2N_{11} + N_{20} + N_{21} + N_{22} + N_{23} + N_{24}) \tag{13}$$

$$n_4 = x_4 + x_{12} + 7x_{13} + x_{14} + 2x_{15} + 6x_{16} + x_{17} + x_{18} + 3x_{19} + x_{24} = \sum X(N_4 + N_{12} + 7N_{13} + N_{14} + 2N_{15} + 6N_{16} + N_{17} + N_{18} + 3N_{19} + N_{24}) \tag{14}$$

The sum of the action concentrations of all structural elements in a slag is equal to 1.

Table 4: Definitions of the parameters of the prediction model

No.	Reaction	ΔG^0 (J/mol) ^{15,16,18}	N_i	x_i
1#	Ca ²⁺ +O ²⁻ =CaO		$N_1 = N_{Ca^{2+}} + N_{O^{2-}} = 2x_1 / \sum X$	$2x_1 = N_1 \sum X$
2#	Mg ²⁺ +O ²⁻ =MgO		$N_3 = N_{Mg^{2+}} + N_{O^{2-}} = 2x_3 / \sum X$	$2x_3 = N_3 \sum X$
3#	SiO ₂		$N_2 = x_2 / \sum X$	$x_2 = N_2 \sum X$
4#	Al ₂ O ₃		$N_4 = x_4 / \sum X$	$x_4 = N_4 \sum X$
5#	(Ca ²⁺ +O ²⁻)+SiO ₂ =CaSiO ₃	-92500-2.5T	$N_5 = K_1 N_1 N_2$	$x_5 = N_5 \sum X$
6#	2(Ca ²⁺ +O ²⁻)+SiO ₂ =Ca ₂ SiO ₄	-118800-11.3T	$N_6 = K_2 N_1^2 N_2$	$x_6 = N_6 \sum X$
7#	3(Ca ²⁺ +O ²⁻)+SiO ₂ =Ca ₃ SiO ₅	-118800-6.7T	$N_7 = K_3 N_1^3 N_2$	$x_7 = N_7 \sum X$
8#	(Mg ²⁺ +O ²⁻)+SiO ₂ =MgSiO ₃	-41100+6.1T	$N_8 = K_4 N_2 N_3$	$x_8 = N_8 \sum X$
9#	2(Mg ²⁺ +O ²⁻)+SiO ₂ =Mg ₂ SiO ₄	-67200+4.31T	$N_9 = K_5 N_2 N_3^2$	$x_9 = N_9 \sum X$
10#	(Ca ²⁺ +O ²⁻)+Al ₂ O ₃ =CaO·Al ₂ O ₃	-18000-18.83T	$N_{10} = K_6 N_1 N_4$	$x_{10} = N_{10} \sum X$
11#	12(Ca ²⁺ +O ²⁻)+7Al ₂ O ₃ =12CaO·7Al ₂ O ₃	-86100-205.1T	$N_{11} = K_7 N_1^{12} N_4^7$	$x_{11} = N_{11} \sum X$
12#	3(Ca ²⁺ +O ²⁻)+Al ₂ O ₃ =3CaO·Al ₂ O ₃	-12600-24.69T	$N_{12} = K_8 N_1^3 N_4$	$x_{12} = N_{12} \sum X$
13#	(Ca ²⁺ +O ²⁻)+2Al ₂ O ₃ =CaO·2Al ₂ O ₃	-16700-25.52T	$N_{13} = K_9 N_1 N_4^2$	$x_{13} = N_{13} \sum X$
14#	(Ca ²⁺ +O ²⁻)+6Al ₂ O ₃ =CaO·6Al ₂ O ₃	-16380-37.58T	$N_{14} = K_{10} N_1 N_4^6$	$x_{14} = N_{14} \sum X$
15#	2(Ca ²⁺ +O ²⁻)+Al ₂ O ₃ +SiO ₂ =2CaO·Al ₂ O ₃ ·SiO ₂	-61964.64-60.29T	$N_{15} = K_{11} N_1^2 N_2 N_4$	$x_{15} = N_{15} \sum X$
16#	(Ca ²⁺ +O ²⁻)+Al ₂ O ₃ +2SiO ₂ =CaO·Al ₂ O ₃ ·2SiO ₂	-13816.44-55.266T	$N_{16} = K_{12} N_1 N_2^2 N_4$	$x_{16} = N_{16} \sum X$
17#	3Al ₂ O ₃ +2SiO ₂ =3Al ₂ O ₃ ·2SiO ₂	-8600-17.41T	$N_{17} = K_{13} N_2^2 N_4^3$	$x_{17} = N_{17} \sum X$
18#	(Ca ²⁺ +O ²⁻)+(Mg ²⁺ +O ²⁻)+2SiO ₂ =CaO·MgO·SiO ₂	-124766.6+3.768T	$N_{18} = K_{14} N_1 N_2 N_3$	$x_{18} = N_{18} \sum X$
19#	3(Ca ²⁺ +O ²⁻)+(Mg ²⁺ +O ²⁻)+2SiO ₂ =3CaO·MgO·2SiO ₂	-315469+24.786T	$N_{19} = K_{15} N_1^3 N_2^2 N_3$	$x_{19} = N_{19} \sum X$
20#	(Ca ²⁺ +O ²⁻)+(Mg ²⁺ +O ²⁻)+2SiO ₂ =CaO·MgO·2SiO ₂	-80387-51.916T	$N_{20} = K_{16} N_1 N_2^2 N_3$	$x_{20} = N_{20} \sum X$
21#	2(Ca ²⁺ +O ²⁻)+(Mg ²⁺ +O ²⁻)+2SiO ₂ =2CaO·MgO·2SiO ₂	-73688-63.639T	$N_{21} = K_{17} N_1^2 N_2^2 N_3$	$x_{21} = N_{21} \sum X$
22#	(Mg ²⁺ +O ²⁻)+Al ₂ O ₃ =MgO·Al ₂ O ₃	-35600-2.09T	$N_{22} = K_{18} N_3 N_4$	$x_{22} = N_{22} \sum X$

N_i – the mass action concentration of component i ; x_i – the mole number of component i ; $\sum X$ – the total equilibrium mole number of all structural units

$$N_1 + N_2 + N_3 + N_4 + N_5 + N_6 + N_7 + N_8 + N_9 + N_{10} + N_{11} + N_{12} + N_{13} + N_{14} + N_{15} + N_{16} + N_{17} + N_{18} + N_{19} + N_{20} + N_{21} + N_{22} = 1 \quad (15)$$

The following four formulas can be obtained by combining Equations (11)–(15).

$$N_1 + N_2 + N_3 + N_4 + K_1 N_1 N_2 + K_2 N_1^2 N_2 + K_3 N_1^3 N_2 + K_4 N_2 N_3 + K_5 N_2 N_3^2 + K_6 N_1 N_4 + K_9 N_1 N_4^2 + K_{10} N_1 N_4^6 + K_{11} N_1^2 N_2 N_4 + K_{12} N_1 N_2^2 N_4 + K_{13} N_2^2 N_4^3 + K_{14} N_1 N_2 N_3 + K_{15} N_1^3 N_2^2 N_3 + K_{16} N_1 N_2^2 N_3 + K_{17} N_1^2 N_2^2 N_3 + K_{18} N_3 N_4 - 1 = 0 \quad (16)$$

$$K_{10} N_1 N_4^6 + 2K_{11} N_1^2 N_2 N_4 + K_{12} N_1 N_2^2 N_4 + K_{14} N_1 N_2 N_3 + 3K_{15} N_1^3 N_2^2 N_3 + K_{16} N_1 N_2^2 N_3 + 2K_{17} N_1^2 N_2^2 N_3 - n_1 (N_2 + K_1 N_1 N_2 + K_2 N_1^2 N_2 + K_3 N_1^3 N_2 + K_4 N_2 N_3 + K_{11} N_1^2 N_2 N_3 + 2K_{12} N_1 N_2^2 N_4 + 2K_{13} N_2^2 N_4^3 + K_{14} N_1 N_2 N_3 + 2K_{15} N_1^3 N_2^2 N_3 + 2K_{16} N_1 N_2^2 N_3 + 2K_{17} N_1^2 N_2^2 N_3) = 0 \quad (17)$$

$$n_3 (0.5N_1 + K_1 N_1 N_2 + 2K_2 N_1^2 N_2 + 3K_3 N_1^3 N_2 + K_6 N_1 N_4 + 12K_7 N_1^{12} N_4^7 + 3K_8 N_1^3 N_4 + K_9 N_1 N_4^2 + K_{10} N_1 N_4^6 + 2K_{11} N_1^2 N_2 N_4 + K_{12} N_1 N_2^2 N_4 + K_{14} N_1 N_2 N_3 + 3K_{15} N_1^3 N_2^2 N_3 + K_{16} N_1 N_2^2 N_3 + 2K_{17} N_1^2 N_2^2 N_3) - n_1 (0.5N_3 + K_4 N_2 N_3 + 2K_5 N_2 N_3^2 + K_{14} N_1 N_2 N_3 + K_{15} N_1^3 N_2^2 N_3 + K_{16} N_1 N_2^2 N_3 + K_{17} N_1^2 N_2^2 N_3 + K_{18} N_3 N_4) = 0 \quad (18)$$

$$n_4 (0.5N_1 + K_1 N_1 N_2 + 2K_2 N_1^2 N_2 + 3K_3 N_1^3 N_2 + K_6 N_1 N_4 + 12K_7 N_1^{12} N_4^7 + 3K_8 N_1^3 N_4 + K_9 N_1 N_4^2 + K_{10} N_1 N_4^6 + 2K_{11} N_1^2 N_2 N_4 + K_{12} N_1 N_2^2 N_4 + K_{14} N_1 N_2 N_3 + 3K_{15} N_1^3 N_2^2 N_3 + K_{16} N_1 N_2^2 N_3 + 2K_{17} N_1^2 N_2^2 N_3) - n_1 (N_4 + K_6 N_1 N_4 + 7K_7 N_1^{12} N_4^7 + K_8 N_1^3 N_4 + 2K_9 N_1 N_4^2 + 6K_{10} N_1 N_4^6 + K_{11} N_1^2 N_2 N_4 + K_{12} N_1 N_2^2 N_4 + 3K_{13} N_2^2 N_4^3 + K_{18} N_3 N_4) = 0 \quad (19)$$

Hence, the equation group of Equations (16)–(19) represents the developed thermodynamic model for calculating mass action concentrations of the structural units or ion couples from the CaO-SiO₂-MgO-Al₂O₃ slags equilibrated with hot metal.

3.3 Sulphide-capacity model based on the IMCT

To date, a series of experimental and theoretical studies has been carried out to determine the sulphur distribution ratio for different slag systems of binary and multi-components. The desulphurization reactions between CaO-SiO₂-MgO-Al₂O₃ slags and metal can be presented as follows:

$$(Ca^{2+}+O^{2-})+[S]=(Ca^{2+}+S^{2-})+[O] \quad (20)$$

$$\Delta G^\theta=105784.6 - 28.723T \text{ (J/mol)}^{20}$$

$$K_{CaS} = \frac{a_{CaS} a_O}{a_{Ca} a_S} = \frac{N_{CaS} a_O}{N_{Ca} a_S} = \left(\frac{2(\%S)_{CaS} / M_S}{\sum n_i} \right) [\%O] f_O = \frac{(\%S)_{CaS} [\%O]}{16N_{CaS} [\%S] \sum n_i} \times \frac{f_O}{f_S}$$

$$L_{S,CaO} = \frac{(\%S)_{CaS}}{[\%S]} = \frac{16K_{CaS} N_{CaO} \sum n_i}{[\%O]} \times \frac{f_S}{f_O} \quad (22)$$

$$(Mg^{2+}+O^{2-})+[S]=(Mg^{2+}+S^{2-})+[O] \quad (23)$$

$$\Delta G^\theta=203604.6 - 35.023T \text{ (J/mol)}^{20}$$

$$K_{MgS} = \frac{a_{MgS} a_O}{a_{MgO} a_S} = \frac{N_{MgS} a_O}{N_{MgO} a_S} = \left(\frac{2(\%S)_{MgS} / M_S}{\sum n_i} \right) [\%O] f_O = \frac{(\%S)_{MgS} [\%O]}{16N_{MgO} [\%S] \sum n_i} \times \frac{f_O}{f_S}$$

$$L_{S,MgO} = \frac{(\%S)_{MgS}}{[\%S]} = \frac{16K_{MgS} N_{MgO} \sum n_i}{[\%O]} \times \frac{f_S}{f_O} \quad (25)$$

Therefore, the total sulphur distribution ratio between CaO-SiO₂-MgO-Al₂O₃ slags and metal can be described as follows:

$$L_S = L_{S,CaO} + L_{S,MgO} = \frac{(\%S)_{CaS+MgS}}{[\%S]} = \frac{(\%S)_{CaS} + (\%S)_{MgS}}{[\%S]} = \frac{16(K_{CaS} N_{CaO} + K_{MgS} N_{MgO}) \sum n_i}{[\%O]} \times \frac{f_S}{f_O} \quad (26)$$

[%O] is the concentration of oxygen in the molten iron, f_S is the Henrian activity coefficient of the sulphur dissolved in the hot metal, f_O is the Henrian activity coefficient of the oxygen dissolved in the hot metal. The oxygen activity in the hot metal can be calculated by choosing the equilibrium of CO/C pairs.¹⁵

The sulphur distribution between slag and metal can be correlated with the sulphide capacity by combining Equations (9) and (26). Therefore, the sulphide capacity can also be written as follows:

$$\lg C_s = \lg L_s - \lg f_s + \frac{1210}{T/K} - 5.814 \quad (27)$$

The activity coefficient of sulphur in the metal can be calculated as follows:

Table 5: Experimental data and sulphide capacities of CaO-SiO₂-MgO-Al₂O₃ slags

No.	Slag compositions/mass%				R /-	w(MgO)/w(Al ₂ O ₃) /-	tested	IMCT model	Sommerville's model	KTH model
	CaO	SiO ₂	MgO	Al ₂ O ₃						
1#	47.02	36.17	4.8	12	1.30	0.40	-2.504	-2.588	-3.644	-3.635
2#	44.65	34.34	6.0	15	1.30	0.40	-2.577	-2.585	-3.419	-3.802
3#	42.27	32.52	7.2	18	1.30	0.40	-2.664	-2.596	-3.361	-3.493
4#	40.69	31.30	8.0	20	1.30	0.40	-2.744	-2.590	-3.362	-3.419
5#	35.85	34.14	10.0	20	1.05	0.50	-2.859	-2.716	-3.533	-3.39
6#	37.51	32.49	10.0	20	1.15	0.50	-2.72	-2.605	-3.063	-3.35
7#	38.89	31.11	10.0	20	1.25	0.50	-2.643	-2.486	-3.988	-2.935
8#	40.21	29.78	10.0	20	1.35	0.50	-2.537	-2.385	-3.074	-3.741
9#	42.39	32.60	5.0	20	1.30	0.25	-2.829	-2.675	-3.473	-3.013
10#	41.26	31.73	7.0	20	1.30	0.35	-2.738	-2.617	-2.743	-2.859
11#	40.13	30.86	9.0	20	1.30	0.45	-2.693	-2.571	-3.377	-3.004
12#	39.00	30.00	11.0	20	1.30	0.55	-2.592	-2.532	-2.498	-3.784

$$\lg f_i = \sum_j e_i^j [%j] \tag{28}$$

Where e_s^j is the interaction parameter of species j on S in the molten iron, [% i] is the concentration of element in the hot metal. The interaction parameters are shown in Table 1.

4 DISCUSSION

4.1 Results of the calculated sulphide capacity for CaO-SiO₂-MgO-Al₂O₃ slags and hot metal

Table 5 shows the results of the sulphur capacity measured by testing CaO-SiO₂-MgO-Al₂O₃, the sulphur capacity predicted by the ion and molecule coexistence theory, the sulphur capacity calculated by Sommerville's model and the sulphur capacity calculated by the KTH model. Figure 4 shows the comparison of the sulphur capacity measured with the CaO-SiO₂-MgO-Al₂O₃ test, the sulphur capacity predicted by the ion and molecule coexistence theory, the sulphur capacity calculated by Sommerville's model and the sulphur capacity calculated by the KTH model. The present data is in good agreement with that predicted by Sommerville's model, KTH model and IMCT model, and the IMCT model is the closest to the present work. The calculation of error (Equation (29)) shows that the relative error of the sulphur capacity predicted by the ion and molecule coexistence theory (4 %) is lower than that calculated by Sommerville's model (23 %) and KTH model (26 %). To further verify the reliability of the model, the literature reference values are compared with the sulphur capacity predicted by the ion and molecule coexistence theory, Sommerville's model and the KTH model, as shown in Figure 5. It can be seen from Figure 5 that the sulphur capacity predicted by the ion and molecule coexistence theory has a good linear relationship with the reference sulphur capacity, and the relative error is the smallest. Therefore, the theoretical model of ion and molecule co-

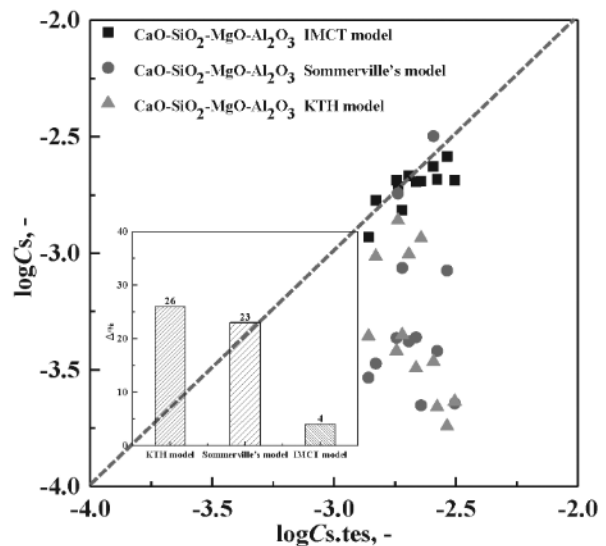


Figure 4: Comparison of the experimental values with the model-calculated sulphide capacity

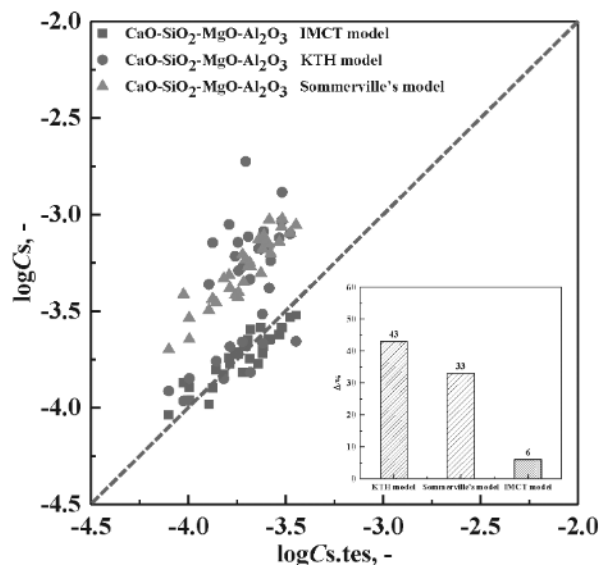


Figure 5: Comparison of literature reference sulphur capacities with the model-calculated sulphide capacity⁷

existence can be used to calculate the sulphur capacity of the CaO-SiO₂-MgO-Al₂O₃ quaternary slag system.

$$\Delta = \frac{1}{n} \times \sum_{i=1}^n \frac{\lg C_{s,i} - \lg C_{s,tes,i}}{\lg C_{s,tes,i}} \times 100 \% \quad (29)$$

4.2 Effect of R on the sulphide capacity of CaO-SiO₂-MgO-Al₂O₃ slags

Figure 6 shows the effect of R on the sulphide capacity of the CaO-SiO₂-MgO-Al₂O₃ slags at 1773 K under each condition. When Al₂O₃ is 20 w/% and w/% (MgO)/w/% (Al₂O₃) = 0.5, the sulphide capacity increases with the increase in R. The increase in alkalinity means that the relative content of CaO increases, providing more (O²⁻). On the other hand, with the increase in R, the SiO₂ networks are modified into smaller anion groups and the proportion of free oxygen ions increases. According to the theory of ion and molecule coexistence, the increase in the O²⁻ activity in a solution is conducive to the forward reaction (Ca²⁺ + O²⁻) + [S] = (Ca²⁺ + S²⁻) + [O]. Therefore, the sulphide capacity increased with the increase in R.

4.3 Effect of w(MgO)/w(Al₂O₃) on the sulphide capacity of CaO-SiO₂-MgO-Al₂O₃ slags

Figure 7 shows the effect of w/% (MgO)/w/% (Al₂O₃) on the sulfide capacity of the CaO-SiO₂-MgO-Al₂O₃ slags at 1773 K under each condition. When Al₂O₃ is 20 w/% and R = 1.30, the sulphide capacity increases with the increase in w/% (MgO)/w/% (Al₂O₃). With the increase in w/% (MgO)/w/% (Al₂O₃), the content of CaO and SiO₂ decreases and the MgO content increases, causing a decrease in O²⁻ from CaO, but the increase in MgO can partially substitute CaO, providing O²⁻ for desulphurization. According to the theory of ion and molecule coexistence, an increase in the O²⁻ activity in a solution is conducive to the forward reaction (Mg²⁺ +

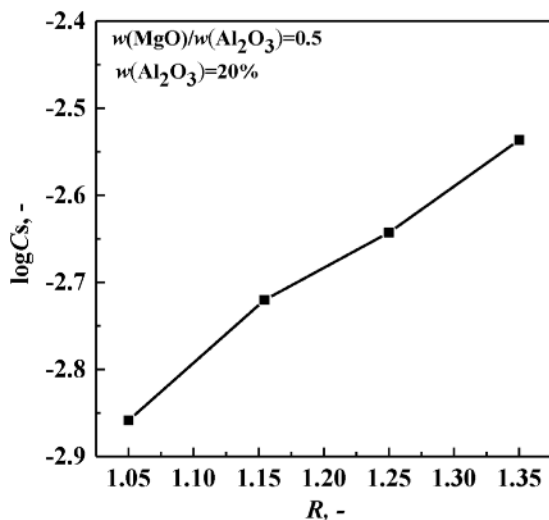


Figure 6: Effect of R on the sulphide capacity of the slags at 1773 K

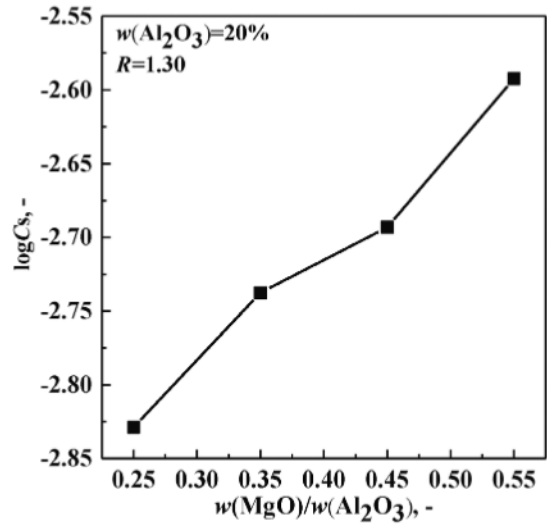


Figure 7: Effect of w/% (MgO)/w/% (Al₂O₃) on the sulfide capacity of the slags at 1773 K

O²⁻) + [S]=(Mg²⁺ + S²⁻) + [O]. MgO has a dilution effect on the slag,²⁰ which can effectively improve the fluidity of the slag and the dynamic conditions of slag desulfurization, thereby improving the desulfurization ability of the slag. With the increase in the MgO content, free oxygen ions are provided. The complex Si-O bond is broken due to the interaction with bridge oxygen, and the SiO₄⁴⁻ and AlO₄⁵⁻ bonds are also broken,^{21,22} thus simplifying the slag network structure. Therefore, the sulphide capacity increases with the increase in w/% (MgO)/w/% (Al₂O₃).

4.4 Effect of Al₂O₃ w/% on the sulphide capacity of CaO-SiO₂-MgO-Al₂O₃ slags

Figure 8 shows the effect of Al₂O₃ w/% on the sulphide capacity of the CaO-SiO₂-MgO-Al₂O₃ slags at 1773K under each condition. When R = 1.30 and w/% (MgO)/w/% (Al₂O₃) = 0.40, the sulphide capacity decreases with the increase in w/% (Al₂O₃). Al₂O₃ has a high affinity with O²⁻ ions, and the reaction generates (Al_xO_y)^{z-} composite anions, thus reducing the concentration of O²⁻ ions in the slag, preventing the transfer of O²⁻ ions to the iron solution and inhibiting the transfer of [S] from the iron solution to the slag. Under the experimental conditions, Al³⁺ in the slag replaces Si⁴⁺ to form AlO₄⁵⁻. In this process, Al-O contributes to the formation of a tetrahedral unit similar to SiO₄⁴⁻, thus forming a more complex aluminosilicate structure²¹ and deteriorating the desulfurization conditions. Therefore, the sulphide capacity decreases with the increase in Al₂O₃ w/%.

5 CONCLUSIONS

A sulphide-capacity prediction model of CaO-SiO₂-MgO-Al₂O₃ slags was developed based on the ion and molecule coexistence theory (IMCT). This was verified using experimentally determined sulphur capacities, and

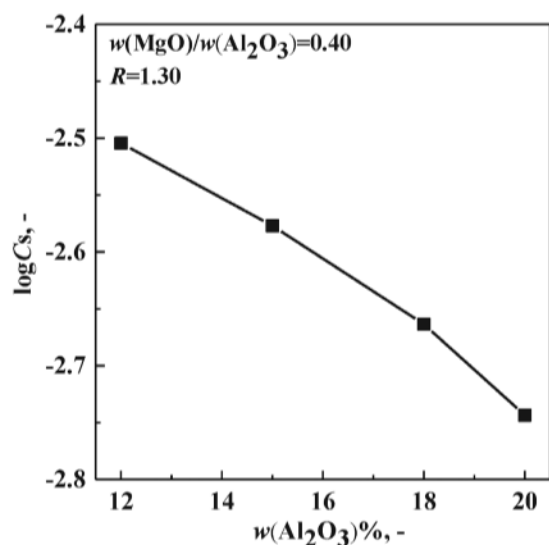


Figure 8: Effect of Al₂O₃ w% on the sulphide capacity of the slags at 1773 K

the effects of R ($w(\text{CaO})/w(\text{SiO}_2)$), $w(\text{MgO})/w(\text{Al}_2\text{O}_3)$ and $w(\text{Al}_2\text{O}_3)$ on the sulphur capacities were discussed. The main conclusions are as follows:

There is a good linear relationship between the experimental values and predicted values. Therefore, the theoretical model of molecular ion coexistence can be used for calculating the sulphur capacity of a CaO-SiO₂-MgO-Al₂O₃ quaternary slag system. When Al₂O₃ is 20 w% and $w(\text{MgO})/w(\text{Al}_2\text{O}_3) = 0.5$, the sulphide capacity increases with the increase in R . When Al₂O₃ is 20 w% and $R = 1.30$, the sulphide capacity increases with the increase in $w(\text{MgO})/w(\text{Al}_2\text{O}_3)$. When $R = 1.30$ and $w(\text{MgO})/w(\text{Al}_2\text{O}_3) = 0.40$, the sulphide capacity decreases with the increase in Al₂O₃ w%.

Acknowledgement

The authors wish to acknowledge the contributions by the associates and colleagues from the Northeastern University of China. This research was financially supported by the National Natural Science Foundation of China (NSFC51774071, NSFC52074072, NSFC51974073, NSFC52074074, NSFC52074086).

6 REFERENCES

- Zhang, X. Lv, Z. Yan, Desulphurisation ability of blast furnace slag containing high Al₂O₃ and 5 mass% TiO₂ at 1773 K, *Ironmak. Steelmak.*, 43 (2016) 5, 378–384, doi:10.1080/03019233.2015.1104070
- J. H. Park, G. Park, Sulfide capacity of CaO-SiO₂-MnO-Al₂O₃-MgO slags at 1873 K, *ISIJ Int.*, 52 (2012) 5, 764–769
- M. M. Nzotta, S. C. Du, S. Seetharaman, Sulphide capacities in some multi component slag systems, *ISIJ Int.*, 38 (1998) 11, 1170–1179, doi:10.2355/isijinternational.38.1170

- Z. T. Zhang, G. H. Wen, P. Tang, The influence of Al₂O₃/SiO₂ ratio on the viscosity of mold fluxes, *ISIJ Int.*, 48 (2008) 6, 739–746, doi:10.2355/isijinternational.48.739
- A. Shankar, G. Mårten, S. Seetharaman, Sulfide capacity of high alumina blast furnace slags, *Metall. Mater. Trans. B*, 37 (2006) 6, 941–947, doi:10.1007/BF02735016
- M. Andersson, P. G. Jonsson, M. M. Nzotta, Application of the sulphide capacity concept on high-basicity ladle slags used in bearing-steel production, *Transactions of the Iron & Steel Institute of Japan*, 39 (1999) 11, doi:10.2355/isijinternational.39.1140
- X. D. Ma, M. Chen, H. F. Xu, Sulphide capacity of CaO-SiO₂-Al₂O₃-MgO system relevant to low MgO blast furnace slags, *ISIJ Int.*, 56 (2016) 12, 2126–2131, doi:10.2355/isijinternational. ISIJINT-2016-274
- X. D. Ma, M. Chen, J. Zhu, Properties of low-MgO ironmaking blast furnace slags, *ISIJ Int.*, 58 (2018) 8, 1402–1405, doi:10.2355/isijinternational. ISIJINT-2018-022
- J. D. Seo, S. H. Kim, Sulphide capacity of CaO-SiO₂-Al₂O₃-MgO-(FeO) smelting reduction slags, *Steel Res Int.*, 70 (1999) 6, 203–208, doi:10.1002/srin.199905627
- R. W. Young, J. A. Duffy, G. J. Hassall, Use of optical basicity concept for determining phosphorus and sulphur slag-metal partitions, *Ironmak. Steelmak.*, 19 (1992) 3, 201–219
- N. J. Sosinsky, I. D. Sommerville, The composition and temperature dependence of the sulfide capacity of metallurgical slags, *Metall. Mater. Trans. B*, 17 (1986) 2, 331–337, doi:10.1007/BF02655080
- S. C. Du, R. S. Nilsson, S. Seetharaman, A mathematical model for estimation of sulphide capacities of multi-component slags, *Steel Res. Int.*, 66 (1995) 11, 458–462, doi:10.1002/srin.199501155
- M. M. Nzotta, S. C. Du, S. Seetharaman, A study of the sulfide capacities of iron-oxide containing slags, *Metall. Mater. Trans. B*, 30 (1999) 50, 909–920, doi:10.1007/s11663-999-0096-4
- R. G. Reddy, M. Blander, Modeling of sulfide capacities of silicate melts, *Metall. Mater. Trans. B*, 18 (1987) 3, 591–596, doi:10.1007/BF02654272
- X. M. Yang, J. S. Jiao, R. C. Ding, A thermodynamic model for calculating sulphur distribution ratio between CaO-SiO₂-Al₂O₃-MgO ironmaking slags and carbon saturated hot metal based on the ion and molecule coexistence theory, *ISIJ Int.*, 49 (2009) 12, 1828–1837, doi:10.2355/isijinternational.49.1828
- C. B. Shi, X. M. Yang, J. S. Jiao, A sulphide capacity prediction model of CaO-SiO₂-Al₂O₃-MgO ironmaking slags based on the ion and molecule coexistence theory, *ISIJ Int.*, 50 (2010) 10, 1362–1372, doi:10.2355/isijinternational.50.1362
- A. Shankar, Sulphur partition between hot metal and high alumina blast furnace slag, *Ironmak. Steelmak.*, 33 (2006) 5, 413–418, doi:10.1179/174328106X113968
- J. Zhang, Computational thermodynamics of metallurgical melts and solutions, Metallurgical Industry Press, Beijing 2007, 245
- M. Allibert, H. Gaye, *Slag Atlas*, 2nd ed., Verlag Stahleisen GmbH: Düsseldorf, Germany 1995, 28, 39, 44, 88, 103, 134
- X. Yuan, J. L. Zhang, R. Mao, Effect of $w(\text{MgO})/w(\text{Al}_2\text{O}_3)$ ratio on desulfurization capacity of BF slag, *Journal of Northeastern University (Natural Science)*, 36 (2015) 11, 1609–1613, doi:10.3969/j.issn.1005-3026.2015.11.020
- J. H. Park, D. J. Min, H. S. Song, Amphoteric behavior of alumina in viscous flow and structure of CaO-SiO₂(-MgO)-Al₂O₃ slags, *Metall. Mater. Trans. B*, 35 (2004) 2, 269–275, doi:10.1007/s11663-004-0028-2
- H. Kim, W. H. Kim, I. Sohn, The effect of MgO on the viscosity of the CaO-SiO₂-20wt%Al₂O₃-MgO slag system, *Steel Res. Int.*, 81 (2010) 4, 261–264, doi:10.1002/srin.201000019